Burr removal from measurement data of honeycomb core surface based on dimensionality reduction and regression analysis

OPEN ACCESS
IOP Publishing
Measurement Science and Technology
Meas. Sci. Technol. **29** (2018) 115010 (11pp)
https://doi.org/10.1088/1361-6501/aae1c4

Burr removal from measurement data of honeycomb core surface based on dimensionality reduction and regression analysis

Yan Qin[1], Renke Kang[1], Zhigang Dong[1,3], Yidan Wang[1], Jie Yang[2] and Xianglong Zhu[1]

[1] Key Laboratory for Precision and Non-traditional Machining of Ministry of Education, Dalian University of Technology, Dalian 116024, People's Republic of China
[2] School of Mathematical Sciences, Dalian University of Technology, Dalian 116024, People's Republic of China

E-mail: dongzg@dlut.edu.cn

Received 19 March 2018, revised 3 September 2018
Accepted for publication 17 September 2018
Published 18 October 2018

Abstract

The quantitative evaluation of the shape accuracy of the machined honeycomb cores has always been difficult, due to its typical thin-wall and low-rigidity characteristics. Laser triangulation is adopted in this paper to measure the surface shape of honeycomb cores due to its advantages of high-accuracy and high-speed, but the original measurement is not accurate enough as a result of the inclusive massive burr data. This paper presents an approach to remove burr data of each extracted cell wall based on dimensionality reduction and regression analysis. First, according to their distribution characteristics, burr data are divided into two types: burr I data and burr II data. Second, vertical and horizontal dimensionality reduction, respectively used for removing burr I data and burr II data, are applied to the measured data to reduce the dimension from three to two. Finally, in the 2D space after dimensionality reduction, the distribution line of the cell wall is forecasted with regression analysis, and burrs are removed according to its distance to the distribution line. Experimental results show that the proposed method has an outstanding performance in removing burr data on various shapes of surfaces.

Keywords: measurement of honeycomb core, burr removal, dimensionality reduction, regression analysis

(Some figures may appear in colour only in the online journal)

1. Introduction

Honeycomb core, as the core component of a composite sandwich structure, is widely used in engineering applications including aviation, aerospace, automotive, ships, and high-speed trains [1–3] due to its high strength-to-weight ratio. Error in the processing of honeycomb cores causes the delamination of sandwich structures, which are sufficiently troublesome to cause concern. For closer control over the accuracy of machining quality, precision measurement of honeycomb cores plays a crucial role [4–6].

Among all kinds of honeycomb cores, Nomex honeycomb core is the most commonly used core material in industrial applications, which is composed of adhered strips of Nomex paper. A Nomex honeycomb core is a kind of cellular material that is composed of interconnected hexagonal cells with the

[3] Author to whom any correspondence should be addressed.

size of each unit cell 2–5 mm and the wall thickness about 0.05–0.2 mm [7]. The thin-wall and low-rigidity characteristics make it difficult to measure with contact instruments. Although the contact probe can be adapted by increasing the contact area to locate on cell walls, the deformation of cell walls is hard to be avoided, which bring about the error of measurement results [8, 9]. Therefore, non-contact measurement is more suitable for measuring this material. Stereo vision measurement techniques, based on digital fringe projection and phase-shifting methods, have been widely used in 3D shape measurement [10, 11]. Based on this technology, Jiang *et al* developed a triangular camera-projector layout to achieve the measurement of honeycomb cores, which is combined with the proposed phased-based stereo matching algorithm [12]. However, the adoptive edge data extraction algorithm in the method ignores the influence of burrs; thus, it cannot measure honeycomb cores with burrs precisely.

Therefore, we attempt to measure the honeycomb surface with a linear laser displacement sensor to collect enough data points on the hyper-thin cell wall [13]. For practical application, it is convenient to achieve high-accuracy and high-speed measurement with the linear laser displacement sensor driven by a numerical control machine tool. Moreover, such high-resolution measurement only generates a small amount of data from the cell wall edges, since the inside of honeycomb cells are hollow. However, when laser triangulation achieves precise measurement on the cell wall edges, burrs are also measured and contained in the measurement result. Burrs on cell walls cannot be thoroughly avoided on the machined surface due to the surface characteristic of Nomex honeycomb cores [14–16], but their height values deviate from cell wall data, which will influence the further analysis and evaluation of the measured surface. As a consequence, a method for removing burr data from the measurement result is highly in demand.

After finishing high-resolution measurement of honeycomb cores, its subsequent data processing is still difficult. Directly processing multiple unit cells to remove burrs is very painstaking. Therefore, we have proposed a cell wall detection method for recognizing all the cell walls one by one, where data of each cell wall can be extracted in order to be processed individually [13]. Although the processing of the measured data has been converted to the processing of each cell wall data, it is still difficult to remove the burr data. The data of honeycomb cell wall is quite limited due to its poor thickness, while burr data are quite a few. In this case, both the shape of the cell wall and the distribution of its height are varied for the same honeycomb core, instead of being a fixed shape. Moreover, the distribution forms of burrs on cell walls include lumpy, threadlike forms, or dots right on the cell wall. The size and direction of burrs are both variant, which make their removal complicated. Because such distribution is different from noise caused by external disturbance, the removal of burrs cannot use traditional filter-denoising methods [17]. For some denoising method applied in laser scanning point cloud, the curvature is usually undertaken to analyze the noise [18, 19], which is not suitable for such discontinuous honeycomb structure.

This paper proposes an approach for removing burr data from each cell wall data based on dimensionality reduction and regression analysis. Section 2 presents the overview of the method including the classification of burrs, and the introduction of dimensionality reduction and regression analysis. The concrete implementation of these two approaches is detailed in section 3. Section 4 presents the experimental results. Finally, conclusions are drawn in section 5.

2. Overview of the method

Based on the cell wall detection method in [13], the data of each cell wall are extracted successively, which are the processing object of the method in this paper. Firstly, according to the distribution position, burrs are divided into two types: burr I and burr II (in section 2.1). Then reduce a vertical dimension of the measured data to obtain a 2D space (vertical dimensionality reduction), where burr I data are identified with regression analysis, thereby removed from the measured data. After burr I data are removed, a horizontal dimension of the remaining measured data is reduced to acquire another 2D space (horizontal dimensionality reduction), where burr II data are identified, and thus removed from the remaining measured data. Among these processes, the adopted dimensionality reduction and regression analysis methods are introduced in sections 2.2 and 2.3, while the detailed procedures of the method are described in section 3.

2.1. Classification of burrs

This paper investigates Nomex honeycomb core material, which is fabricated from Nomex paper using adhesive bonding. Nomex paper is made up of aromatic polyamide (aramid) fibers immersed in resin, whose length and direction are variant. The fibers are of high strength, and are difficult to be thoroughly cut off during the machining process, which will produce different forms of burrs on the machined surface [20]. There mainly exist three geometrical shapes, as illustrated in figure 1.

2.1.1. Lumpy burr. One form of burrs is lumpy. A lumpy burr appears when the marginal fibers of the cutting chip are not thoroughly cut off, which will attach the cutting chip with the cell wall. The width of some lumpy burrs may be several times of the cell wall.

2.1.2. Threadlike burr. Some burrs are threadlike, which are formed when some fibers are not cut off in time but are directly pulled out in the machined section during the machining process. Such burrs are thin with long or short length, and their entire areas are very small.

2.1.3. Dotted burr. The left burrs are dotted, which correspond to the unstable measured data on cell walls due to the roughness of honeycomb cores.

In consequence, it is obvious that burrs have various sizes. The smallest one is only as small as a dot, while the biggest

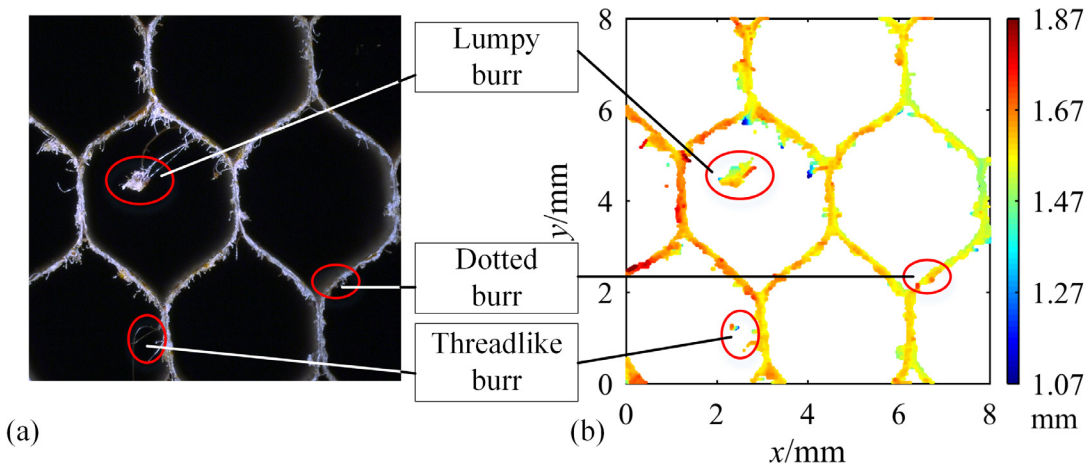

Figure 1. Illustrations of different types of burrs: (a) plan view of honeycomb core; (b) the corresponding measurement result (different colors indicate the wall heights).

one possesses several times the width of the cell wall. Besides, the distribution directions of burrs change disorderly in 3D space. These two characteristics make it difficult for the three types of burrs to be recognized specifically.

Therefore, aiming at simplifying the removal process of burrs, this paper classifies all burrs into two types according to their position. Burrs that can be seen in the plan view are defined as burr I, including the threadlike burrs and lumpy burrs except the parts right above the cell wall. The remainder are burrs whose projection on the plan view is located on the cell wall, which causes that they cannot be seen on the plan view, and are defined as burr II. Burr II includes dotted burrs and the parts of the threadlike burrs and lumpy burrs exactly right on the cell wall.

After being classified, the two types of burr data can be removed based on their different characteristics: burr I data exist in the inside of the honeycomb cells, while burr II data possess different heights with normal cell wall data. Based on these characteristics, burr I can be recognized according to the cell wall distribution in the plan view, and burr II can be detected by the height distribution. However, if burr II data are firstly removed, burr I data will interfere with the recognition of normal cell wall data by the height distribution, due to their deviant heights and large amount. For this reason, burr II data are processed after burr I data are removed.

2.2. Dimensionality reduction

Dimensionality reduction is a process of reducing the dimension number of data [21]. The measured data of honeycomb cores are 3D, where burrs are very difficult to be removed, because of the complication of their distribution directions. Therefore, this paper does not directly deal with the measured data, but reduces its dimension number from three to two in order to reduce the difficulty of recognizing burrs from the measured data. In this study, dimensionality reduction is achieved by projecting the measured data into a plane to acquire the wanted 2D data [22]. Then, burrs will be recognized in the projection plane and then removed in the original measured data accordingly.

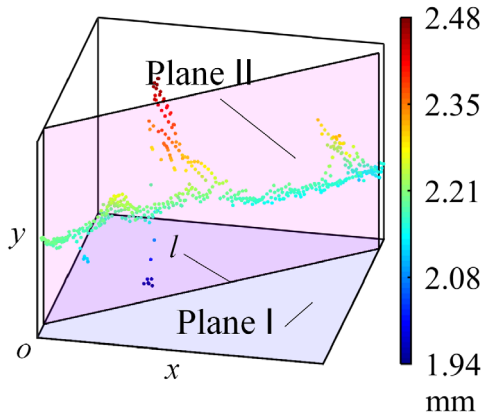

Figure 2. Schematic of projection planes.

Firstly, vertical dimensionality reduction is employed on the measured data to remove burr I data, and then after burr I data are removed, horizontal dimensionality reduction will be employed to remove burr II data. In the process of vertical dimensionality reduction, the top view plane of the measured data is taken as the projection plane (plane I figure 2). As for horizontal dimensionality reduction, the projection plane is the one (plane II in figure 2) that is perpendicular to plane I and its projection line (l in figure 2) in plane I is the approximate line of the cell wall data. In the 2D space after each time of dimensionality reduction, the distribution line of the cell wall can be obtained, while burrs obviously deviate from the line. By this principle, burrs can be recognized in order to be removed from the original measured data.

2.3. Regression analysis

After dimensionality reduction, in the 2D space of the measured data, the distribution of the cell wall is considered to be close to a straight line or a curve with a certain width. Once the distribution line of the cell wall is determined, burr data can be recognized by analyzing the distance between itself to the distribution line, if the distance is larger than the set threshold, the data will be regarded as burr data.

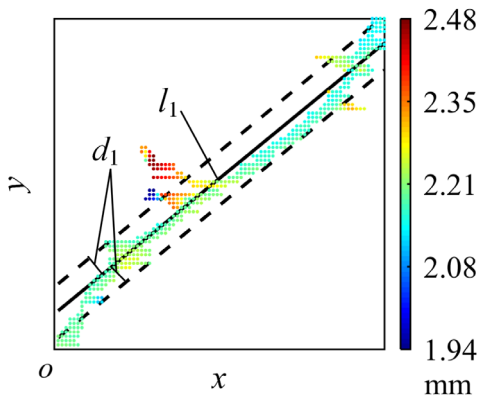

Figure 3. Coarse removal of burr I data using linear regression model.

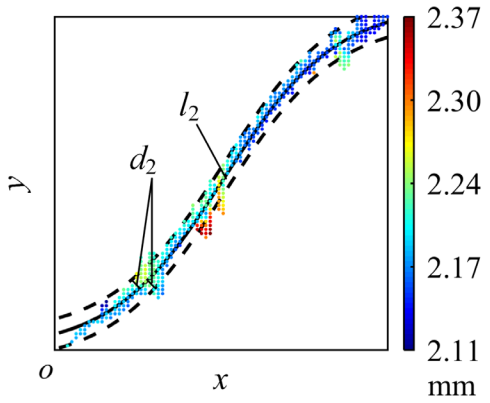

Figure 4. Fine removal of burr I data using non-linear regression model.

However, the shape and position of the distribution line are indefinite, so its concrete mathematic function is also unknown. After observation on burrs, it is found that although some burrs are large in size, their positions are far from cell walls; Some are near to cell walls, but occupy small area. Therefore, the distribution line can be forecasted with regression analysis to fit the data using linear or non-linear function [23, 24]. The precision of regression analysis is affected by burr data, and the more burr data there are, the larger deviation there would be. As a result, regression analysis is repeatedly used to gradually approximate the true distribution line with the decrease of burr data, while the threshold for recognizing burr data is reduced gradually.

3. Description of the method

In this paper, the removal of burr data was realized through programming on Matlab R2018a programming software. During the implementation of above methods, the key techniques are the process of projecting the measured data into a plane, the determination of regression models, and the determination of thresholds. All these will be specified in this section.

3.1. Removal of burr I data

Burr I data are identified in the 2D space acquired through vertical dimensionality reduction, and then be removed from the measured data with regression analysis. Furthermore, the removal of burr I data is broken down into two procedures in order to achieve more accurate burr removal result, which are coarse and fine removal.

During vertical dimensionality reduction, the projection plane (plane I) is the *xoy* plane, and the result of every data point after dimensionality reduction is its *x*-coordinate and *y*-coordinate, as shown in figure 3. In the acquired 2D space, the actual distribution of the cell wall is a curve not a straight line. Non-linear regression model should be adopted to fit the curve, but it is greatly influenced by burr data. For this reason, in the coarse removal, linear regression model is taken for removing the majority of burr I data (l_1 in figure 3). Then in the fine removal, specific non-linear regression model (l_2 in figure 4), corresponding to the actual distribution of the cell wall, is adopted for removing the remainder burr I data. Once the distribution line is determined, burr data can be recognized by analyzing the distance between itself to the distribution line. If the distance is larger than the set threshold (such as d_1 in figure 3 and d_2 in figure 4), the data will be regarded as burr data.

(1) Coarse removal. Fit the dimension-reduced measured data with the linear regression model [25]:

$$f(t) = \alpha_1 + \alpha_2 t. \tag{1}$$

The variable t is considered to be an explanatory variable, while $f(t)$ is considered to be a dependent variable. α_1 and α_2 are the parameters to be estimated. It is reasonable to take the axis who has the longer range as the explanatory variable for cell walls of different directions. Then parameters α_1 and α_2 can be determined automatically with the help of regression analysis tools in Matlab. The determination of other parameters used in the regression below is in the same way, and will not be stated again.
In order to improve the accuracy of burr removal, regression analysis is used repeatedly (at least three times are recommended) with the thresholds gradually decreasing, in which only part of burr data is removed each time. Besides, in the coarse removal stage, the threshold of last regression analysis is a little larger than half of the width of the cell wall.

(2) Fine removal. For further fine removal, the actual distribution of the cell wall is taken into consideration. Besides, cell walls of different directions should be processed separately, due to their different distributions. The actual distribution of double cell wall data for all honeycomb cores is a straight line, while most of single cell walls are curves. In order to describe these different distributions, the available regression models includes.

3.1.1. Linear regression model. For all double cell walls, their fine removals take the linear regression that is same with

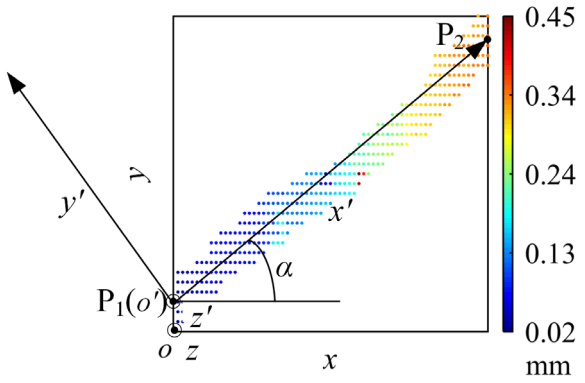

Figure 5. The determination of projection plane II.

equation (1). Moreover, linear regression model is also suitable for single cell walls of some types of honeycomb cores.

3.1.2. Logistic regression model. For some types of honeycomb cores, the actual distribution of single cell wall data is close to 'S' shape, which can be expressed with logistic function [26]. The regression model is the logistic function:

$$f(t) = \frac{L}{1 + e^{-k(t-t_0)}}. \tag{2}$$

The variable t is considered to be an explanatory variable, while $f(t)$ is considered to be a dependent variable. L, k and t_0 are the parameters to be estimated. The data need to be rotated or flipped to be placed with 'S' shape prior to using this regression.

3.1.3. Polynomial regression model. Some single cell walls are neither straight line nor close to 'S' shape. The cell wall may not have a definite shape and is hard to be described uniformly. Such shape can be forecasted with a n-degree polynomial function [27].

$$f(t) = \beta_0 + \beta_1 t^1 + \beta_2 t^2 + \cdots + \beta_n t^n. \tag{3}$$

The variable t is considered to be an explanatory variable, while $f(t)$ is considered to be a dependent variable. β_0, β_1,…, β_n are the parameters to be estimated. Once the number of degree is determined, the polynomial function can be solved with Matlab software. Because of the irregularity of the cell wall shape, it is hard to give the concrete value of n, and 5–10 are recommended.

Similarly, in the fine removal, the remaining burr I data are removed for multiple times with gradually decreasing thresholds, where the threshold of last regression analysis is half of the width of the cell wall.

3.2. Removal of burr II data

After burr I data are removed, to remove burr II data from the remaining measured data, horizontal dimensionality reduction is employed to obtain a 2D space, where burr II data are identified with regression analysis, and removed from the remaining measured data. Similar with the removal of burr I, the removal of burr II data also contains two procedures, which are coarse and fine removal.

During horizontal dimensionality reduction, to determine plane II, the approximate line of the cell wall in plane I is firstly determined by fitting the x-coordinate and y-coordinate of the measured data to a straight line, as shown in figure 5, where $P_1(x_1, y_1)$ and $P_2(x_2, y_2)$ are the intersection points of the line and the two axes, and α is its inclination angle. To achieve dimensionality reduction, a new coordinate system o'-x'y′z′ is established with x'-axis along the approximate line. The coordinate components of any points in coordinate system o'-$x'y'z'$ can be transferred and expressed in coordinate system o-xyz through coordinate transformation in equation (4):

$$\begin{bmatrix} x' \\ y' \\ z' \end{bmatrix} = T \begin{bmatrix} x - x_1 \\ y - y_1 \\ z \end{bmatrix}. \tag{4}$$

Where $T = \begin{bmatrix} \cos(\alpha) & \sin(\alpha) & 0 \\ -\sin(\alpha) & \cos(\alpha) & 0 \\ 0 & 0 & 1 \end{bmatrix}$ is the transformation matrix.

In coordinate system o'-$x'y'z'$, the result of every data point after dimensionality reduction is its x'-coordinate and z'-coordinate, as shown in figure 6, where plane II has been moved for a certain distance along y'-axis to make the schematic clearly. The distribution line (l_3 in figure 6) of the cell wall after dimensionality reduction reflects the height fluctuation of cell wall data. Then to identify and remove burr II data, the corresponding regression model is used for expressing the line. Taking x' as the explanatory variable, and z' as the dependent variable, the relationship between them can be expressed with a function (the concrete function is specified in its concrete removal stage):

$$z' = f(x'). \tag{5}$$

From equations (4) and (5), the fitted value on the projection plane that every data point corresponds to is:

$$z_i' = f(x_i') = f((x_i - x_1)\cos(\alpha) + (y_i - y_1)\sin(\alpha)). \tag{6}$$

The deviation between actual measured value and the fitted value is:

$$\Delta h = |z_i - z_i'|. \tag{7}$$

Then remove the measured data whose Δh is greater than the set threshold h.

The removal of burr II data also contains two procedures of coarse and fine removal.

(1) Coarse removal. In this stage, the selected regression model is a linear regression model.
Here, part of burr II data are removed for multiple times with gradually decreasing thresholds, where the threshold of last regression analysis is a little larger than half of the height fluctuation range of cell wall data.
(2) Fine removal. For honeycomb cores, the measured result represents its micro profile, which is irregular and hard

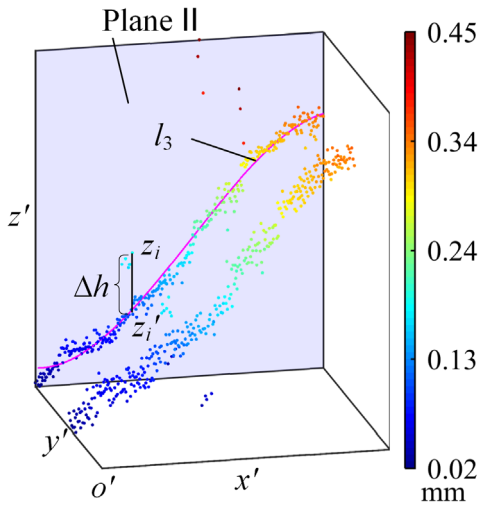

Figure 6. Removal of burr II data using non-linear regression model.

to be expressed with an exact shape. In this situation, polynomial regression analysis is suitable for describing the distribution thanks to its superior flexibility.

Similarly, the remaining burr II data are removed for multiple times with gradually decreasing thresholds, where the threshold of last regression analysis is half of the height fluctuation range of cell wall data.

In the different removal stage of burrs (coarse or fine removal) for removing different type of burrs (burr I or burr II), the suitable regression models are different. In summary, only linear regression is used in coarse removal, while the alternative regression models in the fine removal of burr I contain linear regression model, logistic regression model, and polynomial regression model, and only polynomial regression model is suitable for the fine removal of burr II. Because the cell walls of the same direction in a honeycomb core use the same regression model, only if all of them accord with identical shape, the corresponding regression model will be adopted. Otherwise, polynomial regression model is appropriate owing to its stronger adaptation.

3.3. Determination of thresholds

As stated above, in every stage, burrs are removed repeatedly, corresponding to a set of thresholds, respectively. Each threshold can be expressed as a multiple of the final data band width w_0, where w_0 is the cell wall width when removing burr I, and is the height fluctuation range when removing burr II. Each set of thresholds can be determined by considering the following factors:

3.3.1. The number of repetitions. The more the repetitions are, the closer the regression analysis result gets to the true distribution of the cell wall and the more computation time it will consume at the same time. According to our tests, five times for coarse removal and three times for fine removal are suitable, because the further increase of repetitions brings no evident improvement of the result but an increase of computation time.

Table 1. Main specifications of linear laser displacement sensor.

Parameters	Value
Measurement range of z-axis (height)	± 8 mm (F.S. $= 16$ mm)
Measurement range of x-axis (width)	15 mm
Repeatability	0.4 μm
Linearity	$\pm 0.1\%$ F.S.
Light source	405 nm blue semiconductor laser
Spot shape	Approx. 21 mm $\times$ 45 μm
Reference distance	60 mm
Sampling frequency	Max. 16 μs

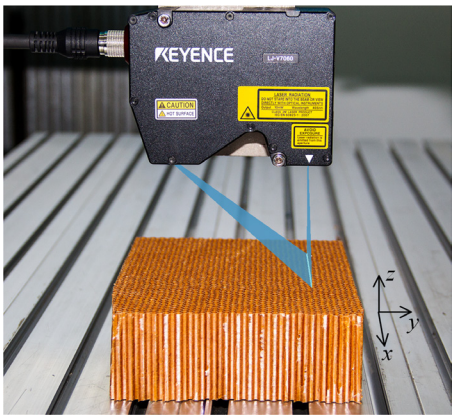

Figure 7. Laser measurement schematic.

3.3.2. The order of thresholds. The thresholds in each set are descending. Every time regression analysis is used, burr data are reduced a little. With the decrease of burr data, the line of regression analysis gets closer to the true distribution line, which requires descending thresholds.

3.3.3. The last threshold. The final remaining data at each burr removal stage depend on the last threshold. For this reason, the last threshold of fine removal, as the last time of burr removal, is determined as 0.5 w_0. Since the final remaining data of coarse removal still contain some burrs, the last threshold related with the data band width should be a little larger than 0.5 w_0. Additionally, 0.75 w_0 is found to have an excellent effect for its ability to remove burrs around the cell wall.

3.3.4. The first threshold. Before burrs are removed, the result of the initial regression analysis deviates far from the true distribution of cell walls; thus, the corresponding threshold should be chosen large enough to only remove distant burrs. On the other hand, from coarse removal to fine removal, as linear regression analysis changes to non-linear, the same threshold might lead to a sudden increase of removing burrs, which results in lower burr removal accuracy. Therefore, in order to remove burrs at a steady speed, the first threshold of fine removal is chosen a little larger than the last threshold of coarse removal.

Table 2. Regression models of different cell walls.

	Coarse removal of burr I	Fine removal of burr I	Coarse removal of burr II	Fine removal of burr II
Double cell wall	Linear regression	Linear regression	Linear regression	Quintic polynomial regression
Single cell wall	Linear regression	Quintic polynomial regression	Linear regression	Quintic polynomial regression

Table 3. Thresholds in regression analysis.

Coarse removal of burr I	Fine removal of burr I	Coarse removal of burr II	Fine removal of burr II
$[5d_0, 2.5d_0, 1.5d_0, d_0, 0.75d_0]$	$[d_0, 0.75d_0, 0.5d_0]$	$[5h_0, 2.5h_0, 1.5h_0, h_0, 0.75h_0]$	$[h_0, 0.75h_0, 0.5h_0]$

3.3.5. The threshold interval. The threshold intervals in each set are in declining trend. In this way, the speed of removing burrs can be reduced, which can improve the burr removal accuracy.

4. Experiment verification

The proposed burr removal method is suitable for processing 3D measurement data of honeycomb cores from any achievable measurement mean. This paper only takes laser measurement data as an example for the validation and analysis of the method. The proposed method is programmed with MATLAB R2018a software for display and rendering on three honeycomb core specimens.

4.1. Experiment apparatus

A linear laser displacement sensor (LJ-V7060, Keyence, Japan) was used for the measurement. Its specifications are summarized in table 1. During measuring, the incident laser was set along the cell wall, as shown in figure 7. The laser probe was mounted on a three-axis numerical control machine tool for scanning the surface of the specimen that was fixed to the workbench. The resolution of the measured data is 20 μm $\times$ 25 μm.

4.2. Parameters

The proposed method mainly depends on the regression models and the thresholds in different burr removal stages. These options are identical for the three specimens in this paper. According to different suitable regression models in the different removal stage for removing different type of burrs, the selected regression models are shown in table 2. After observation, the cell wall distribution fluctuate not very strongly, and quintic polynomial regression is close to the distribution. Such selection is also suitable for most measurement results except those whose cell walls correspond to specific regression models.

Table 3 presents the thresholds that are successively used in regression analysis of every burr removal stage, where d_0 and h_0 are the cell wall width and the height fluctuation range, respectively. The values of d_0 and h_0 are consistent for the same type of honeycomb cores. Considering the selection principle in section 3.3, both burr I data and burr II data are removed for five times of coarse removal and three times of fine removal, with thresholds of descending values and intervals. In coarse removal, the first thresholds are determined as $5d_0$ and $5h_0$, while the last ones are $0.75d_0$ and $0.75h_0$. In fine removal, the first thresholds are chosen as d_0 and h_0, while the last ones are $0.5d_0$ and $0.5h_0$. Then the thresholds in each burr removal stage can be determined as in table 3. Besides, the given sets of thresholds are effective on most of the measurement results in practical application.

4.3. Results

To evaluate the effectiveness of the proposed burr removal method, experiments were carried out on a flat surface (figure 8), an inclined surface (figure 9) and a curved surface (figure 10), respectively. The honeycomb cores with flat surface and curved surface share the same cell size of 3.2 mm, while the cell size of the inclined honeycomb core is 4.8 mm. The three specimens are the ones without serious lattice deformation, severe burr level or cell wall laceration, and surface quality like these is usually visually inspected in production currently. The objective of this study is to evaluate the surface shape accuracy not the surface quality, so burr data are removed from the measurement result before calculating the surface shape accuracy.

Regarding the tests on real measured data, accurate quantitative evaluations are not possible, since it is very difficult to judge whether a data point in the critical zone is a burr datum or a cell wall datum, owing to the roughness of cell walls. Alternatively, visual observations and descriptive statistics are employed for comparison before and after burr data are removed.

Cell wall detection is firstly employed on the measurement result, and then each detected cell wall is processed by the burr removal method successively. Accordingly, burrs on the whole measured honeycomb surface can be removed. To watch the burr removal results clearly, only a part of the measured surface is shown in the experiment results. Figures 8(c)–10(c) show the measurement results, then figures 8(d)–10(d) present the results of burr I data being removed, and burr II data are removed as shown in figures 8(e)–10(e).

For descriptive statistics, the root-mean-square deviation (RMSD) of a cell wall, referring to the dispersion level of the measure data, is specified as

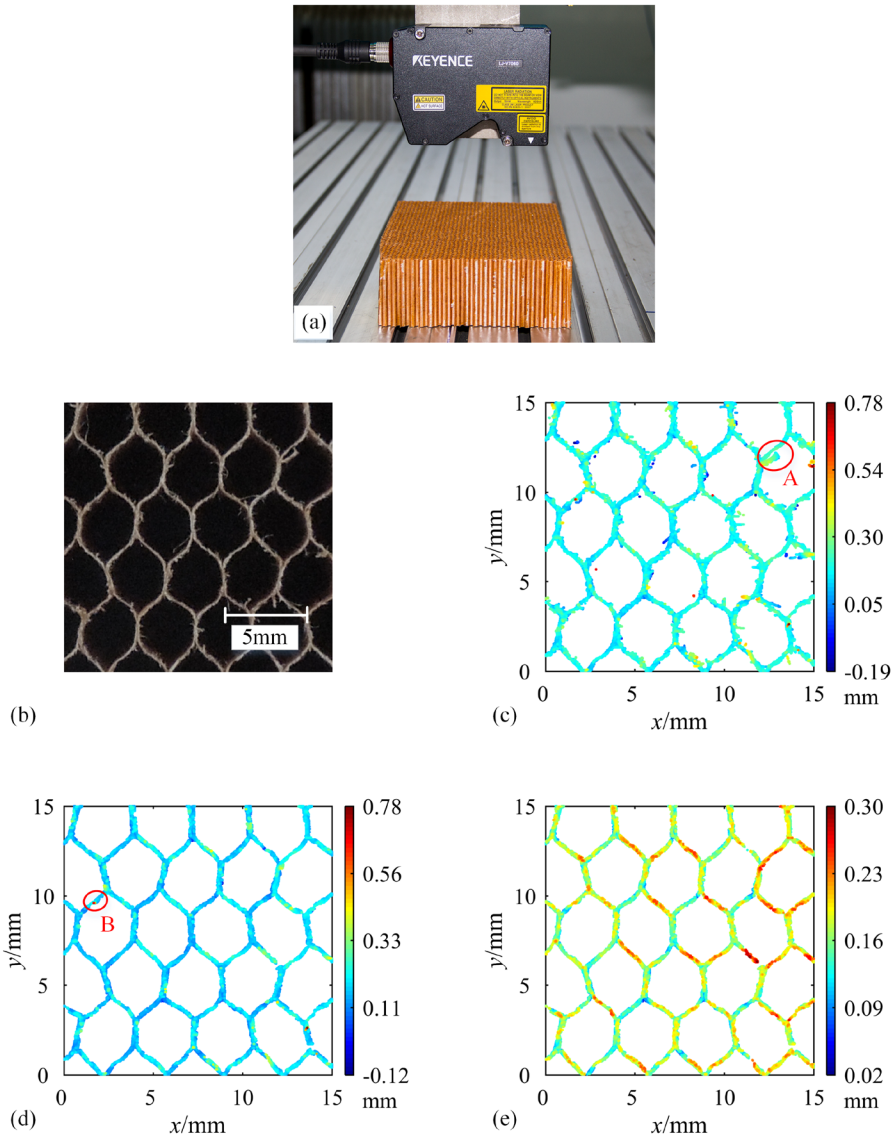

Figure 8. Experimental setup and results of the flat honeycomb core: (a) experimental setup; (b) the plan view; (c) the measurement result; (d) the result of burr I removal; (e) the result of burr II removal.

$$\mathrm{RMSD} = \sqrt{\frac{1}{n}\sum_{t=1}^{n}(p_t - p_{ft})^2} \tag{8}$$

where, p_t ($t = 1, 2, \ldots, n$) is data to be analyzed. p_{ft}, the corresponding predicted value of p_t, is forecasted with fitting based on the final remaining data. The smaller the RMSD is, the more stabilized the data are.

To demonstrate the performance of the proposed method, we calculate the data removal rate (DRR), and the root-mean-square deviation decline rate (RMSDDR), which are defined as:

$$\mathrm{DRR} = \frac{\mathrm{NOM\text{-}NFR}}{\mathrm{NOM}} \times 100\% \tag{9}$$

$$\mathrm{RMSDDR} = \frac{\mathrm{RMSDOM\text{-}RMSDFR}}{\mathrm{RMSDOM}} \times 100\% \tag{10}$$

where NOM = number of original measured data, NFR = number of final remaining data, RMSDOM = mean RMSD of the original measured data, and RMSDFR = mean RMSD of the final remaining data. The statistical results of the three specimens are shown in table 4.

Figure 8 shows the burr removal results of the flat specimen. In the original measured data (figure 8(c)), there exist lots of burr data, including threadlike burrs, lumpy burrs and dotted burrs, which correspond to the surface of honeycomb cores (figure 8(b)). After before and after contrast, burr data are effectively removed in the final remaining data, while there are no obvious accidentally deletions of cell wall data. Circle A gives an example of a typical burr I, while circle B is a burr II, and both are successfully removed. After burr data are removed (figure 8(e)), the range of data decreases from 0.97 mm to 0.28 mm, and obvious visible burrs no longer exist. As shown in table 4, 24.83% of the original measured data are removed, while the RMSD is reduced by 42.84%.

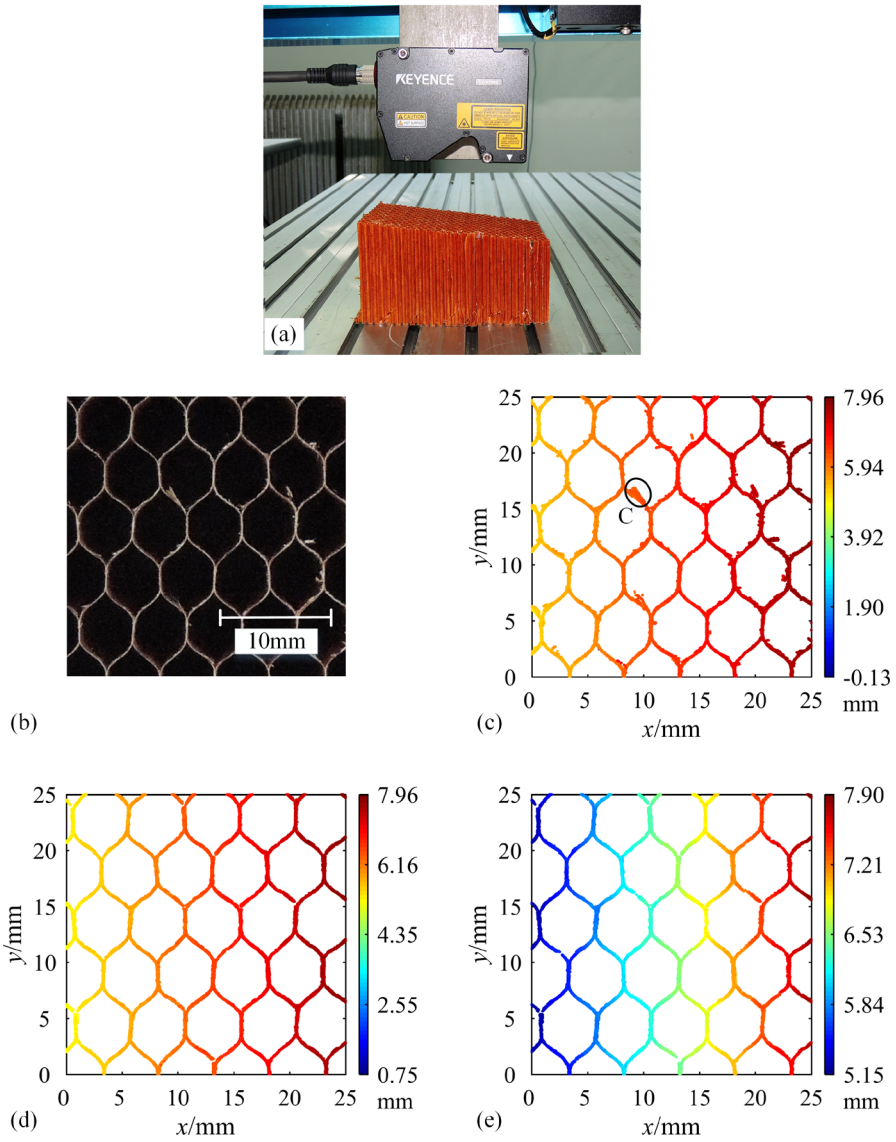

Figure 9. Experimental setup and results of the inclined honeycomb core: (a) experimental setup; (b) the plan view; (c) the measurement result; (d) the result of burr I removal; (e) the result of burr II removal.

The results of the inclined specimen are shown in figure 9. In the aerospace application, inclined surfaces are widely used, thus, the applicability on inclined surfaces for the proposed method is of great practical significance. From figures 9(b) and (c), it can be seen some burrs are near from cell walls, which are considered to be difficult to be removed. As illustrated in circle C, such burr has been successfully removed with the proposed method. The removal of burr data decreases the data range from 8.09 mm to 2.75 mm, corresponding to the height difference of the inclined surface. The percentage of removed data reaches 21.20%, decreasing the RMSD by 65.82%.

We further demonstrated the effectiveness of our burr removal method on the curved surface (figure 10). Despite the more complicated shape, burrs contained in the curved specimen are effectively removed. The curved shape is able to be seen clearly in the final remaining data (figure 10(e)). The removed burr data, accounting for 28.06% of the original measured data, reduce the RMSD by 57.79%.

By comparison between figures 8(c)–10(c) and 8(e)–10(e), it can be found that obvious burr data have been successfully removed. The final remaining data (figures 8(e)–10(e)) are in the form of hexagonal grid, corresponding to the measured surfaces in figures 8(b)–10(b). Besides, the cell wall data are smooth, continuous, and complete, which proves that the majority of the cell wall data are not accidentally removed. Moreover, it can be seen from the results that RMSDFR is much larger than DRR, exhibiting the great improvement on the measured data with the proposed method. Therefore, our method is capable of removing burr data and keeping the cell wall data.

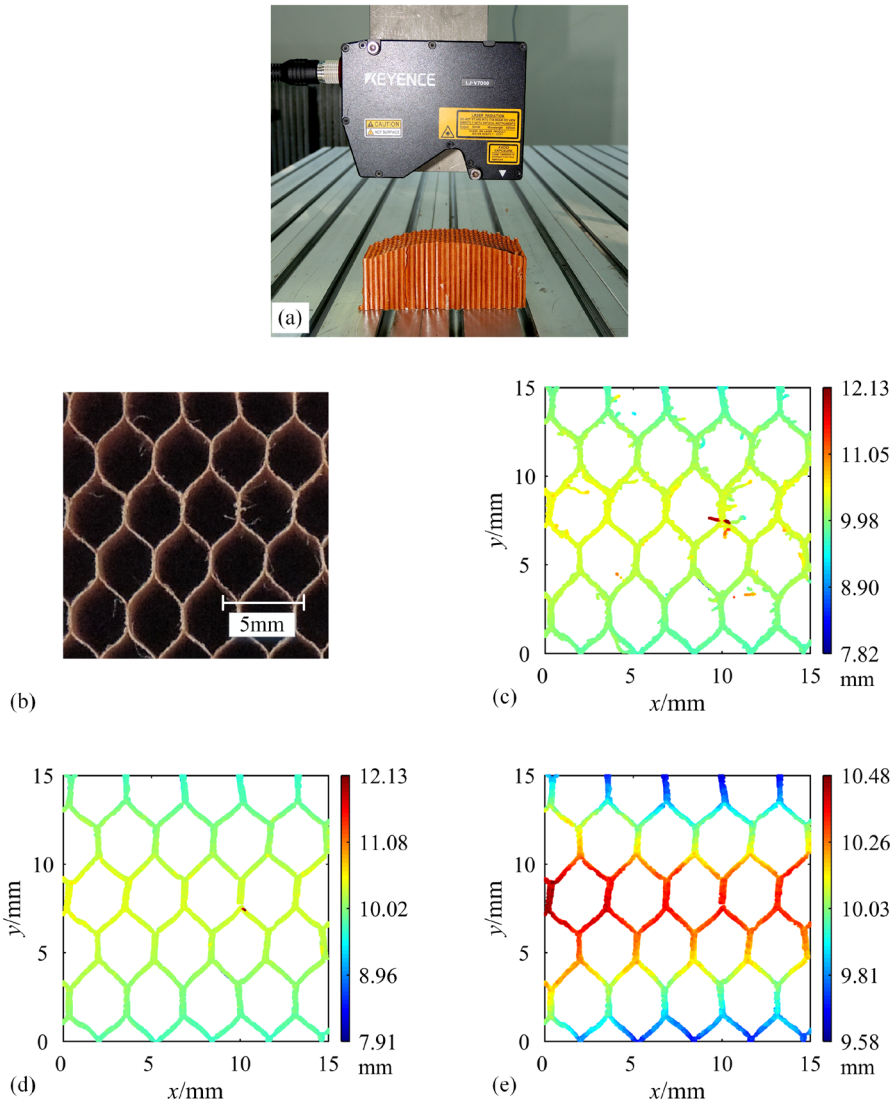

Figure 10. Experimental setup and results of the curved honeycomb core: (a) experimental setup; (b) the plan view; (c) the measurement result; (d) the result of burr I removal; (e) the result of burr II removal.

Table 4. Statistical results of the three specimens.

	NOM	NFR	DRR/%	RMSDOM/mm	RMSDFR/mm	RMSDDR/%
The flat specimen	49 763	37 405	24.83	0.0859	0.0491	42.84
The inclined specimen	73 126	57 620	21.20	0.1188	0.0406	65.82
The curved specimen	63 127	45 413	28.06	0.1059	0.0447	57.79

5. Conclusion

In this paper, we present a method for removing burrs from the measured data of honeycomb cores based on dimensionality reduction and regression analysis. By dimensionality reduction, the dimension of the measured data is reduced from three to two, and then burrs are recognized and removed by regression analysis. The experiments were carried out on flat, inclined and curved surfaces exhibiting the outstanding performance of the proposed method in removing burr data and improving data quality. Then, the surface shape and machining error can be easily computed from the remaining measured data after removing burr data, which is of great significance for guiding machining process and monitoring product quality.

Acknowledgments

The authors would like to acknowledge the financial supports from the Science Fund for Creative Research Groups of NSFC (51621064), the National Science and Technology Major Projects (2016ZX04002005-3), and the National Natural Science Foundation of China (No. 11201051).

ORCID iDs

Yan Qin https://orcid.org/0000-0002-1069-1701
Jie Yang https://orcid.org/0000-0003-1318-3996

References

[1] Seemann R and Krause D 2017 Numerical modelling of Nomex honeycomb sandwich cores at meso-scale level *Compos. Struct.* **159** 702–18
[2] Karakoç A and Freund J 2012 Experimental studies on mechanical properties of cellular structures using Nomex® honeycomb cores *Compos. Struct.* **94** 2017–24
[3] Hu X P, Yu B H, Li X Y and Chen N C 2017 Research on cutting force model of triangular blade for ultrasonic assisted cutting honeycomb composites *Proc. CIRP* **66** 159–63
[4] Kim H Y and Hwang W 2002 Effect of debonding on natural frequencies and frequency response functions of honeycomb sandwich beams *Compos. Struct.* **55** 51–62
[5] Hu X P, Chen S Y and Zhang Z C 2012 Research on curved surface forming of nomex honeycomb material based on ultrasonic NC cutting *Adv. Mater. Res.* **538–41** 1377–81
[6] Menta V G K, Vuppalapati R R, Chandrashekhara K, Pfitzinger D and Phan N 2012 Manufacturing and mechanical performance evaluation of resin-infused honeycomb composites *J. Reinf. Plast. Compos.* **31** 415–23
[7] Liu L, Meng P, Wang H and Guan Z 2015 The flatwise compressive properties of Nomex honeycomb core with debonding imperfections in the double cell wall *Composites* B **76** 122–32
[8] Alblalaihid K, Kinnell P and Lawes S 2015 Fabrication and characterisation of a novel smart suspension for micro-CMM probes *Sensors Actuators* A **232** 368–75
[9] Neamţu C, Hurgoiu D, Popescu S, Dragomir M and Osanna H 2012 Training in coordinate measurement using 3D virtual instruments *Meas. J. Int. Meas. Confed.* **45** 2346–58
[10] Zhao H, Wang Z, Jiang H, Xu Y and Dong C 2015 Calibration for stereo vision system based on phase matching and bundle adjustment algorithm *Opt. Lasers Eng.* **68** 203–13
[11] Liu H, Su W H, Reichard K and Yin S 2003 Calibration-based phase-shifting projected fringe profilometry for accurate absolute 3D surface profile measurement *Opt. Commun.* **216** 65–80
[12] Jiang H, Zhao H, Li X and Quan C 2016 Hyper thin 3D edge measurement of honeycomb core structures based on the triangular camera-projector layout and phase-based stereo matching *Opt. Express* **24** 5502
[13] Qin Y, Dong Z, Kang R, Yang J and Ayinde B 2018 Detection of honeycomb cell walls from measurement data based on Harris corner detection algorithm *Meas. Sci. Technol.* **29** 065004
[14] Song F, Huang G L and Hu G K 2012 Online guided wave-based debonding detection in honeycomb sandwich structures *AIAA J.* **50** 284–93
[15] Grove S M, Popham E and Miles M E 2006 An investigation of the skin/core bond in honeycomb sandwich structures using statistical experimentation techniques *Composites* A **37** 804–12
[16] Roy R, Park S J, Kweon J H and Choi J H 2014 Characterization of Nomex honeycomb core constituent material mechanical properties *Compos. Struct.* **117** 255–66
[17] Sansoni G, Trebeschi M and Docchio F 2009 State-of-the-art and applications of 3D imaging sensors in industry, cultural heritage, medicine, and criminal investigation *Sensors* **9** 568–601
[18] Nurunnabi A, West G and Belton D 2015 Outlier detection and robust normal-curvature estimation in mobile laser scanning 3D point cloud data *Pattern Recognit.* **48** 1400–15
[19] Sun J, Zhang J and Zhang G 2016 An automatic 3D point cloud registration method based on regional curvature maps *Image Vis. Comput.* **56** 49–58
[20] Jaafar M, Atlati S, Makich H, Nouari M, Moufki A and Julliere B 2017 A 3D FE modeling of machining process of Nomex® honeycomb core: influence of the cell structure behaviour and specific tool geometry *Proc. CIRP* **58** 505–10
[21] Tenenbaum J B, deSliva V and Langford J C 2000 A global framework for nonlinear dimensionality reduction *Science* **290** 2319–23
[22] Roweis S T and Saul L K 2000 Nonlinear dimensionality reduction by locally linear embedding *Science* **290** 2323–6
[23] Cleveland W S and Devlin S J 1988 Locally weighted regression: an approach to regression analysis by local fitting *J. Am. Stat. Assoc.* **83** 596–610
[24] Silverman B W 1985 Some aspects of the spline smoothing approach to non-parametric regression curve fitting *J. R. Stat. Soc.* B **47** 1–52
[25] Pérez B, Molina I and Peña D 2013 Outlier detection and robust estimation in linear regression models with fixed group effects *J. Stat. Comput. Simul.* **84** 2652–69
[26] Pardoe I 2004 Model assessment plots for multilevel logistic regression *Comput. Stat. Data Anal.* **46** 295–307
[27] Bickel P J and Li B 2007 Local polynomial regression on unknown manifolds *Complex Datasets Inverse Probl.* **54** 177–86